

Electronic Excitation Energy Transfer between Two Single Molecules Embedded in a Polymer Host

Rémi Métivier,^{1,*} Fabian Nolde,² Klaus Müllen,² and Thomas Basché^{1,†}

¹*Institut für Physikalische Chemie, Johannes Gutenberg-Universität, 55099 Mainz, Germany*

²*Max Planck-Institut für Polymerforschung, 55099 Mainz, Germany*

(Received 19 June 2006; published 25 January 2007)

Unidirectional electronic excitation energy transfer from a photoexcited donor chromophore to a ground state acceptor chromophore—both linked by a rigid bridge—has been investigated by low temperature high-resolution single molecule spectroscopy. Our approach allows for accurately accessing static disorder in the donor and acceptor electronic transitions and to calculate the spectral overlap for each couple. By plotting the experimentally determined transfer rates against the spectral overlap, we can distinguish and quantify Förster- and non-Förster-type contributions to the energy transfer.

DOI: [10.1103/PhysRevLett.98.047802](https://doi.org/10.1103/PhysRevLett.98.047802)

PACS numbers: 78.30.Jw, 33.70.Ca, 33.70.Jg, 34.30.+h

Electronic excitation energy transfer at the single molecule level has been studied both experimentally and theoretically [1–10]. Given typical conditions for experiments in liquid solutions, fluorescence resonance energy transfer (FRET) according to the Förster model [11] after appropriate corrections seems to give a satisfactory description of the transfer process. Accordingly, single pair FRET analysis of donor-acceptor labeled biomolecules has become a powerful tool to obtain information on conformational substates, intermolecular distances, and distance fluctuations [12–15]. In fact, it was shown very recently by sophisticated multiparameter analysis that distance determinations with a precision in the subangstrom regime can be achieved [16].

In solution, it is often assumed that the line shapes are identical for all donors and acceptors yielding a single value for the spectral overlap or derived from this the Förster radius R_0 . Considering energy transfer in solids or frozen solutions, the situation is substantially different, because the spectral overlap between pairs of chromophores with a given orientation and distance will strongly vary due to static disorder or inhomogeneous broadening of the optical transitions involved. Actually, already at the ensemble level Förster theory has to be modified to take properly into account inhomogeneous broadening [17,18]. When analyzing energy transfer at the single molecule level, static disorder inevitably will lead to a distribution of energy transfer rates and efficiencies. Therefore, an ensemble averaged spectral overlap J or Förster radius R_0 will not be a meaningful measure anymore. Yet, as will be shown here, the distribution of spectral overlaps can be quite accurately accessed by interrogating the donor and the acceptor transitions in single molecule experiments at low temperature.

The above considerations hold for multichromophoric aggregates as light-harvesting pigments [2], dendrimers [5], or conjugated polymers [3,19,20], systems of topical interest which recently have been investigated by single

molecule spectroscopy. An additional problem encountered here is the general validity of the Förster model [21,22], because the chromophores may be in close proximity and/or linked by potentially intervening bridge molecules. The corresponding parameters may even not be known accurately as is typically true for conjugated polymers. It has been reported in the literature that under such circumstances the simple dipole approximation may break down or bridge-mediated electronic coupling may contribute to the energy transfer [21–23]. Investigations of single rigid-rod-type conjugated polymer chains seem to be quite controversial in this context, because energy transfer with and without appreciable spectral overlap have been reported [19,20].

To address the issues raised above, we have applied low temperature single molecule spectroscopy to study a well-defined donor (D)-acceptor (A) couple where unidirectional energy transfer occurs after selective donor excitation. The dyad consists of perylene diimide (PDI, D) and terrylene diimide (TDI, A) separated at a fixed distance by a rigid p -terphenyl spacer (Fig. 1). Density-functional theory calculations have found a nearly linear geometry for this dyad. In Fig. 1, the solution ensemble absorption spectra of PDI, TDI, and the dyad are shown. No detectable difference of the absorption spectra of the free and coupled chromophores is observable. Consequently, the coupling between the two chromophores in the dyad is weak.

To conduct the single molecule experiments, thin poly(methyl methacrylate) (PMMA) films (~ 100 nm) containing the dyad at very low concentration, were spin coated on a glass substrate. The samples were transferred into an optical cryostat which allowed confocal imaging of single molecules between room and liquid helium temperatures. To record emission spectra, the samples were excited at 488 nm (Ar-ion laser) or by the output of a tunable ring dye laser (linewidth: ~ 2 GHz). The dye laser was also employed to measure fluorescence excitation spectra. When single dyads were excited at 488 nm (PDI absorption only),

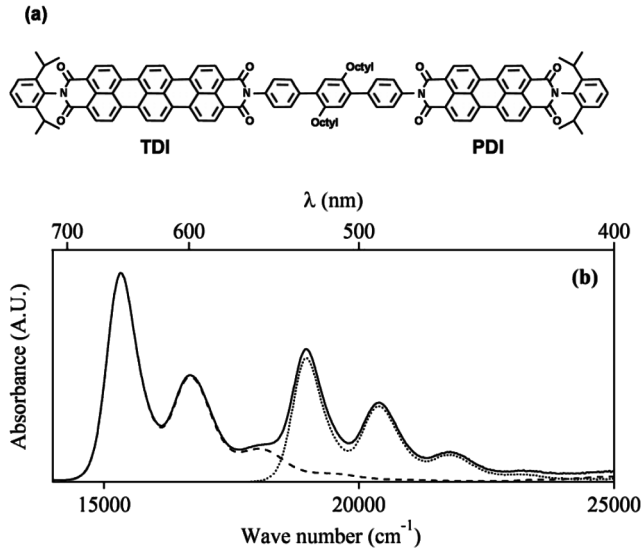


FIG. 1. (a) Chemical structure of the donor (PDI)-acceptor (TDI) dyad with a *p*-terphenyl bridge. (b) Room temperature solution absorption spectra in toluene of PDI (dotted curve), TDI (dashed curve), and the dyad.

at room as well as low temperature (1.4 K), $\sim 85\%$ of the dyads showed TDI emission only, indicating very efficient energy transfer. The remaining percentage is attributed to dyads where premature bleaching of PDI or TDI occurred or where synthesis was incomplete. For further analysis, only dyads were considered in which quantitative excitation energy transfer from the PDI donor to the TDI acceptor was evidenced by pure TDI emission.

As has been shown recently [7], for systems exhibiting weak electron-phonon coupling, the rate constant of energy transfer can be extracted from the widths of the sharp zero-phonon lines observed at low temperatures. In Fig. 2, the fluorescence excitation spectrum of a spatially isolated single dyad in the range of the donor absorption is shown. The spectrum is recorded by scanning the dye laser across the purely electronic [0, 0] transition of PDI while moni-

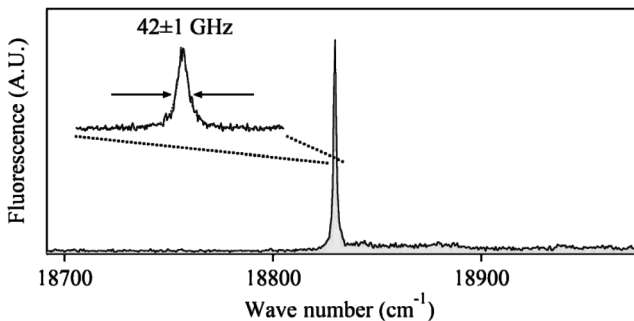


FIG. 2. Fluorescence excitation spectrum of a single dyad at 1.4 K. The enlarged part shows a Lorentzian fit to the data. Linewidths are accessible in the range from 3 up to roughly 500 GHz, corresponding to energy transfer rates between ~ 0.02 and 3 ps^{-1} .

toring the TDI emission. The line shape was fitted to a Lorentzian from which a linewidth of $42 \pm 1 \text{ GHz}$ was obtained. Using the same procedure, we have determined the donor excitation linewidths for 84 single dyads. By varying the excitation intensities ($8\text{--}80 \text{ W/cm}^2$), we verified that the line shapes were not power broadened. In addition, we have measured the linewidth distribution of PDI in PMMA, to determine other contributions to the linewidth as given by the natural lifetime ($\tau_D^0 = 3.8 \text{ ns}$), optical dephasing, and spectral diffusion. The latter distribution yields an average linewidth of 4 GHz for PDI in PMMA, which is clearly smaller than the linewidths (20–110 GHz) found in the PDI excitation spectra of the dyads. Using the relation $\Delta\nu = (2\pi\tau)^{-1}$, we calculate the energy transfer time constants τ_{ET} of the dyads which are plotted in Fig. 4(a). This distribution peaks at around 4 ps, corroborating that energy transfer is indeed very fast.

As pointed out in the introduction, the Förster theory would give a straightforward explanation for such a distribution based on differences in the spectral overlap for each dyad. We stress again that variations of the distance and relative orientation between *D* and *A* are negligible in our dyad. In the Förster rate equation, there is a direct proportionality between the spectral overlap of *D* emission and *A* absorption and the rate constant of energy transfer:

$$k_{ET}^{d-d} = \frac{9000(\ln 10)\kappa^2\Phi_D^0}{128\pi^5 N_A n^4 \tau_D^0 R_{D/A}^6} \int_0^\infty I_D(\lambda)\epsilon_A(\lambda)\lambda^4 d\lambda. \quad (1)$$

The integral in Eq. (1) represents the spectral overlap with a fluorescence intensity of *D* (I_D) and an absorption coefficient of *A* (ϵ_A). The other parameters of Eq. (1) will be discussed below. To get access to the spectral overlaps of the individual dyads, several steps are necessary. First, besides the fluorescence excitation spectra (PDI), we also have measured the fluorescence emission spectra (TDI) for each dyad. These measurements allow us to determine the distributions of purely electronic transition frequencies of PDI and TDI in the dyads [Fig. 3(a)]. A scatter plot of PDI and TDI transition frequencies does not show any correlation. Therefore, for a given dyad in PMMA, the transition frequency of TDI is independent from that of PDI and vice versa.

To calculate the spectral overlap, we need to know the emission spectrum of the donor and the absorption spectrum of the acceptor, too. As donor emission is not observed in the dyads, we have measured the emission spectra of single PDI molecules in PMMA at 1.4 K. Furthermore, we have been able to measure the fluorescence excitation spectra of the TDI acceptor in several single dyads. To do so, we have scanned a dye laser operated with a DCM-SulforhodamineB mixture from ~ 14700 to 16390 cm^{-1} ($\sim 680\text{--}610 \text{ nm}$) while monitoring the redshifted TDI emission. Because of the limited scan range of the dye laser, the complete TDI excitation spectrum could not be measured. Therefore, in addition,

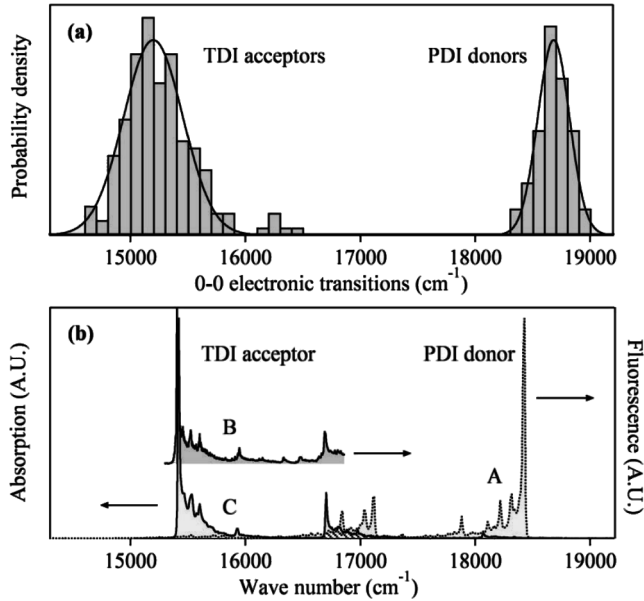


FIG. 3. (a) Inhomogeneous distributions of purely electronic transition frequencies of PDI and TDI. The histograms have been built from emission (TDI part) and excitation (PDI part) spectra of individual dyads at 1.4 K. Gaussian line shapes were fitted to the data. (b) (A) Fluorescence emission spectrum of a single PDI molecule at 1.4 K. (B) Fluorescence excitation spectrum of a single TDI molecule at 20 K. This spectrum originally had been measured in the range 14 850–16 390 cm^{-1} . For emphasizing the D/A -spectral overlap, it has been shifted to higher energies. (C) Simulated absorption spectrum of a single TDI molecule at 1.4 K. The dashed area represents the overlap between donor emission and acceptor absorption.

we simulated the low temperature single molecule excitation spectrum by assuming mirror symmetry with the single molecule emission spectrum. In a further step, we took into account the relative intensity differences between vibronic lines in absorption and emission as determined from the room temperature ensemble solution spectra. In Fig. 3(b), it is seen that the measured and the corresponding part of the simulated excitation spectrum were in excellent agreement, clearly justifying our procedure. To convert the TDI excitation spectrum into an absorption spectrum, we first integrated the S_0 - S_1 room temperature absorption spectrum of TDI in PMMA to get the total absorption cross section (or extinction coefficient). Assuming conservation of oscillator strength, we then calibrated the low temperature absorption spectrum of TDI. Finally, as single molecule spectra do show slight differences in vibronic line intensities from molecule to molecule, we selected the most representative PDI emission and TDI absorption spectra.

In the next step, we computed a full 2D-spectral overlap matrix. The entries of the PDI inhomogeneous distribution (step width: 2.5 cm^{-1}) served as electronic origins of the PDI emission spectrum, while the entries of the TDI dis-

tribution (step width: 4.5 cm^{-1}) served as the electronic origins of the TDI absorption spectrum. A randomly picked realization is displayed in Fig. 3(b). Based upon the lack of correlation between donor and acceptor electronic transitions, the spectral overlaps were calculated between all entries of the PDI and TDI inhomogeneous distributions using the step widths as given above. To convert the distribution of spectral overlaps into a distribution of transfer times, the full fluorescence lifetime distribution of PDI in PMMA was inserted into Eq. (1). The latter distribution, which peaks at $\tau_D^0 = 3.8$ ns and has a width of 0.7 ns, was measured for individual PDI molecules. For the other parameters that appear in Eq. (1), single values were used. Although we have indications for slight deviations from a linear geometry of the dyad [24], the orientation factor κ^2 was set to 4, taking into account that the transition dipoles are oriented along the long molecular axes. $R_{D/A} = 2.8$ nm was determined from the distance between the centers of gravity of the two chromophores. The index of refraction of PMMA is $n = 1.49$, and for the fluorescence quantum yield of PDI the ensemble value in solution was used ($\Phi_D^0 = 1$). The final full probability distribution of energy transfer times τ_{ET} as predicted by Förster theory is plotted in Fig. 4(a). As is immediately evident, there is a substantial discrepancy between the experimental and the calculated distributions. Similar discrepancies based on differences between en-

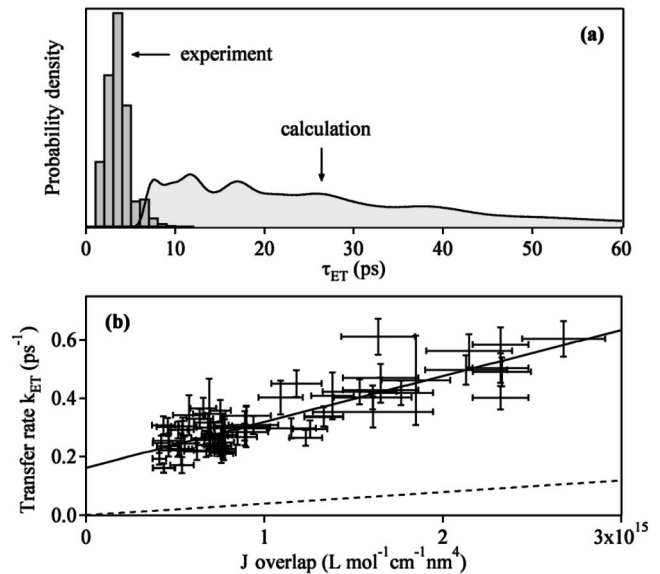


FIG. 4. (a) Distribution of time constants of PDI \rightarrow TDI energy transfer in single dyads as determined by linewidth measurements (gray bars) and full probability distribution of energy transfer times calculated by Förster theory (drawn line, see text for details). (b) Experimentally determined energy transfer rates plotted against the spectral overlap. The dashed line represents the dependency calculated by Förster theory, utilizing a single donor fluorescence lifetime of $\tau_D^0 = 3.8$ ns instead of a distribution.

semble averaged values of the experimental and the calculated (FRET model) energy transfer time constants have been reported for donor-acceptor couples in solution. In particular, recent investigations of porphyrin dimers linked by oligo-*p*-phenyleneethynylene bridges of varying length and chemical composition gave evidence for an additional energy transfer contribution via a bridge-mediated superexchange mechanism [23].

The single molecule experiments presented here further allow for distinguishing the different contributions to the total transfer rate. In Fig. 4(b), we have plotted the experimentally determined energy transfer rates against the spectral overlap, thereby utilizing the unique possibility of single molecule spectroscopy to look for correlations between physical parameters. With increasing spectral overlap, the transfer rate increases linearly, which nicely corroborates a crucial prediction from Förster theory [see Eq. (1)] [25]. Therefore, a Förster-type contribution was not only assumed but actually proven by the data. If solely a FRET mechanism would be operative, the transfer rate should be strictly proportional to the J overlap. In Fig. 4(b), such a linear relationship following the Förster theory is shown, too. In our experiments, however, a clear additional contribution to the energy transfer is observed as a large offset, the magnitude of which increases with increasing spectral overlap. Such dependencies are not accessible in bulk investigations [23], because only average values for the different contributions can be obtained. Therefore, the findings presented here may also serve as an input for advanced theoretical approaches to describe energy transfer beyond the Förster approximation [10]. In addition, our dyad to some extent mimics electronic coupling in conjugated polymers, which are viewed as a collection of chromophoric units separated by chemical defects or less conjugated segments [3]. Consequently, energy transfer seems to occur as hopping of localized excitations, the mechanism of which depends on interchromophoric distances and the nature of the “bridge.”

We thank Mathias Haase for the fluorescence lifetime measurements. This work was supported by the Sonder-

forschungsbereich 625/B6.

*Present address: Laboratoire de Photophysique et Photochimie Supramoléculaire et Macromoléculaire, CNRS UMR8531, Ecole Normale Supérieure de Cachan, 94235 Cachan Cedex, France.

†To whom all correspondence should be addressed.

Electronic address: thomas.basche@uni-mainz.de

- [1] T. Ha *et al.*, Proc. Natl. Acad. Sci. U.S.A. **93**, 6264 (1996).
- [2] A. M. van Oijen *et al.*, Biophys. J. **78**, 1570 (2000).
- [3] J. Yu, D. H. Hu, and P. F. Barbara, Science **289**, 1327 (2000).
- [4] M. Lee, J. Tang, and R. M. Hochstrasser, Chem. Phys. Lett. **344**, 501 (2001).
- [5] M. Cotlet *et al.*, J. Am. Chem. Soc. **125**, 13 609 (2003).
- [6] M. Heilemann *et al.*, J. Am. Chem. Soc. **126**, 6514 (2004).
- [7] R. Metivier *et al.*, J. Am. Chem. Soc. **126**, 14 364 (2004).
- [8] Y. Zhao *et al.*, J. Phys. Chem. B **103**, 3954 (1999).
- [9] S. Jang and R. J. Silbey, J. Chem. Phys. **118**, 9312 (2003).
- [10] S. Jang, M. D. Newton, and R. J. Silbey, Phys. Rev. Lett. **92**, 218301 (2004).
- [11] Th. Förster, Naturwissenschaften **33**, 166 (1946).
- [12] E. A. Lipman *et al.*, Science **301**, 1233 (2003).
- [13] N. K. Lee *et al.*, Biophys. J. **88**, 2939 (2005).
- [14] B. Schuler *et al.*, Proc. Natl. Acad. Sci. U.S.A. **102**, 2754 (2005).
- [15] X. Michalet *et al.*, Annu. Rev. Biophys. Biomol. Struct. **32**, 161 (2003).
- [16] M. Antonik *et al.*, J. Phys. Chem. B **110**, 6970 (2006).
- [17] G. D. Scholes and G. R. Fleming, J. Phys. Chem. B **104**, 1854 (2000).
- [18] K. M. Gaab and C. J. Bardeen, J. Phys. Chem. B **108**, 4619 (2004).
- [19] J. G. Müller *et al.*, Phys. Rev. Lett. **91**, 267403 (2003).
- [20] K. Becker *et al.*, J. Am. Chem. Soc. **128**, 680 (2006).
- [21] S. Speiser, Chem. Rev. **96**, 1953 (1996).
- [22] G. Scholes, Annu. Rev. Phys. Chem. **54**, 57 (2003).
- [23] K. Pettersson *et al.*, J. Phys. Chem. A **110**, 310 (2006).
- [24] C. G. Hübner *et al.*, J. Chem. Phys. **120**, 10 867 (2004).
- [25] R. P. Haugland, J. Yguerabide, and L. Stryer, Proc. Natl. Acad. Sci. U.S.A. **63**, 23 (1969).